Implementation of Novel Carbon Bonded Filter Materials for Steel Melt Filtration – an Overview

M. Emmel, Chr. G. Aneziris

In course of the present work an overview, providing information about the development and characteristic properties of novel active and reactive ceramic foam filter materials for steel melt filtration, is presented. The so-called active filters, based on carbon bonded alumina, are subdivided into an activation due to increased amorphous carbon amounts and an activation due to oxide coatings, whose chemistry equates to that of non-metallic inclusions. These filter types are expected to improve the filtration of especially exogenous, as well as primary and secondary endogenous inclusions. In contrast, the reactive filters, consisting of carbon bonded magnesia, are supposed to decrease the formation of both tertiary and quaternary endogenous inclusions. Here, the carbothermal reduction of the MgO results in gaseous Mg, which reduces the dissolved oxygen in the steel melt. A combination of both filter materials provides the active, as well as the reactive functionality in one filter type. The resulting in situ spinel formation moreover counteracts the shrinkage of the filter material during casting. In collaboration with the industry, testing of a selection of novel filters led to the identification of the influence of the chemistry in filtration processes. Here, alumina coated filters possessed the highest filtration potential.

1 Introduction

Highest demands with regard to performance, reliability and quality of steel castings lead to an increasing pressure on both the metal-making and metal-using industry. In this context, the removal of solid and liquid inclusions such as deoxidation products plays a very special role. It is well known that size, type and distribution of nonmetallic inclusions decrease the mechanical properties and especially the fracture toughness, the tensile strength, the ductility, as well as the fatigue resistance of the cast products dramatically, resulting in excessive casting repairs or rejections [1–5]. In order to remove these nonmetallic inclusions and ensure the requirements of high purity metal castings, ceramic foam filters (CFF) have been used in steel applications for several years. Nowadays, approximately 15 % of the castings are produced by using these filters [6–9]. However, their potential regarding material characteristics and filtration behavior has not been fully exploited yet. Therefore, the Collaborative Research Center 920 (CRC 920) "Multifunctional filters for metal melt filtration – a contribution to zero defect materials" at the Technische Universität Bergakademie Freiberg, in whose framework the current dissertation had been conducted, has set itself the task to improve the filtration behavior of ceramic filter materials. The ambitious aim of a remarkable reduction of nonmetallic inclusions in the metal matrix is to be achieved by the development of both intelligent filter materials and systems. With the aid of functionalized filter surfaces, based on active, ceramic coatings, the deposition of inclusions on the filters is supposed to be improved considerably. In addition, reactive filter materials are intended to react with the dissolved gases in the metal melt, in order to reduce gas impurities, as well as nonmetallic inclusions, which occur below the liquidus temperature. Here, the active filters are based on carbon bonded alumina, which are expected to decrease the amount of exogenous, as well as primary and secondary endogenous inclusions in the steel melt. Therefore, the surface tension at the interfaces filter wall/inclusion/steel melt, are specifically set. On the one hand, this will be carried out by means of the application of oxide coatings, whose chemical composition equates to that of different inclusion types. On the other hand, the functionalization of the active filters should be achieved via increasing amorphous carbon amounts on the surface. The reduction of the amount of dissolved oxygen in the steel melt and hence, decreasing occurrence of endogenous tertiary and quaternary inclusions is aspired with the aid of reactive filters, based on carbon bonded magnesia. Thereby, a reaction of the filter material with

M. Emmel, Chr. G. Aneziris
Technical University Bergakademie Freiberg
Institute of Ceramic, Glass- and Construction Materials
Agricolastraße 17, 09599 Freiberg
Germany

Corresponding author: *M.Emmel*
E-mail: Marcus.Emmel@ikgb.tu-freiberg.de

Keywords: ceramic foam filter, steel melt filtration, carbon bonded oxides

Received: 31.05.2014
Accepted: 23.09.2014

the oxygen is to be caused, resulting in the formation of inclusions, which then deposit on the filter wall. The combination of the active Al_2O_3–C material with the reactive MgO-C should lead to filters, unifying the functionalities of both filter types. Moreover, a possible in situ spinel formation could counteract further shrinkage of the filter material during application, due to the associated volume expansion. Finally, a selection of the newly developed filters is to be tested, in cooperation with the industry, in order to ensure real casting conditions. Besides the applicability of the filters, various parameters are intended to be found, which might give indication of dependencies and processes, occurring in steel melt filtration. Therefore, contaminating filters will be installed in front of the filters to be tested, which impurify the steel melt intentionally. From the use of different contaminating materials, especially the influence of the chemistry on the filtration behavior can be derived.

2 Experimental

The carbon bonded filters were manufactured according to the Schwartzwalder process (replica technique) in two steps [10]. First, a high-viscous impregnating slurry was prepared in a high shear Hobbart-type mixer (ToniTechnik/DE). In the beginning, the respective powder mixtures were dry mixed for 5 min in the mixer. After this step, the additives were dispersed in deionized water and then added to the powder mixture, followed by further additions of deionized water until a plastic mass was formed. This mass was kneaded for additional 5 min. This led to better homogenization and destroyed any agglomerates by shear force. Further additions of deionized water were made, while measuring the viscosity (by means of a hand viscometer Haake/DE), until a value of approximately 600 mPa · s was obtained. The resulting slurry was subsequently used to impregnate PU foamblocks (50 mm × 50 mm × 20 mm). The slurry was hand-pressed into the PU foam to ensure a complete coating of the polyurethane skeleton. In order to create the first coating on the polyurethane skeleton, it was necessary to remove excess impregnating slurry. Therefore, each PU foamblock (filled with slurry) was pressed through a roll-pressing device that consisted of two counter rotating rolls with a diameter of 44 mm. The gap between the rolls was 4 mm and the rotation speed of them was 60 revolutions/min. Subsequently, the impregnated foams were dried for 12 h at 25 °C to a constant weight. During this process step, the generation of unfavourable defects, due to the relaxation of the squeezed foam and drying, were observed in the filters. Note that the desired thickness of the ceramic coating was not easily adjusted under normal processing conditions. Thus, a further step – the spraying of a second ceramic layer – had to be accomplished. Spraying of the dried foams was carried out in a spraying chamber. A spray gun SATAjet B (Sata/DE), with a nozzle diameter of 1,4 mm and a spraying pressure of 3 bar was used. The distance between the nozzle and filter was kept constant at approximately 10 cm. The spraying took place on all 6 sides of the filter. The largest sides, in regard to the surface area, were sprayed for 3 s; and the smaller dimensioned sides, for about 1 s, resulting in a wet filter weight of 26 g. The sprayed samples were subsequently dried again at 25 °C, for 12 h and reweighed. The dried filter was thermally treated by a pyrolysis process, which took place in retorts filled with calcined petcoke (Müco/DE), having a particle size between 0,2–2,0 mm. The final temperature of 800 °C was reached with a heating rate of 1 K/min and a holding time of 180 min. Additional holding time steps of 30 min were adopted every 100 °C, after which the samples being thermally treated were allowed to cool down inside the oven. The compositions of filters and coatings, respectively, are shown in Tab. 1–5. The cold crushing strength (CCS) was determined on a universal testing machine TT 2420 (TIRA GmbH/DE), using a 20 kN pressure cell. The displacement speed was 3 mm/min until a counteracting force of 5 N was reached. At this load, the displacement speed was changed to 1 N/mm²/s. The experiment was terminated when a strength loss of 80 % was reached. Young's modulus of elasticity (E) was determined by impulse excitation technique. Therefore, a rectangular bar is excited by a projectile. Concerning the influence of varying carbon types on the Young´s modulus, filters of 20 mm × 50 mm × 150 mm were tested. Due to the excitation, the sample oscillates and the frequency of this oscillation is measured by a microphone. Via fast Fourier transformation the time dependent signal is converted into a frequency spectrum. The flexural and torsional frequencies were measured in order to obtain Young's modulus of elasticity as well as Poisson's ratio at room temperature. For the characterization of the shrinkage behavior of the oxide coatings, the dilatometer DIL 402 C (Netzsch/DE) was used. The coated, as well as uncoated filter bars, were of the size 5 mm × 5 mm × 20 mm. Except for the coating, the filter substrates were precoked at 800 °C in reducing atmosphere. Under argon atmosphere, the coatings were sintered within the equipment at 1400 °C. Both the heating and the cooling rate amounted to 5 K/min. The so-called impingement test has been accomplished in order to verify the applicability of the newly developed filter materials. Within this test, the cold filters (18 °C) are impinged with approx. 6 kg of steel melt (1670 °C) with a drop height of 30 cm, to evaluate their thermal shock resistance, as well as their permeability. Therefore, filters 50 mm × 50 mm × 20 mm in size have been cemented into the bottom side of a sand mold. For the evaluation of the in situ spinel formation of the new developed combined active and reactive carbon bonded filters a new metal-casting simulator of Systec/DE was used. The complete test for this contribution took place under fully-controlled argon atmosphere. Approximately 30 kg of commercially available 42CrMo4 steel in bars was placed in an alumina/spinel melting crucible. A 10 ppi prismatic carbon bonded filter, based on the template geometry 130 mm × 25 mm × 25 mm, was fixed at a special sample holder in a gas tight sewer port above the melting crucible. After evacuation, the sample was inserted in the steel melt and rotated with 30 revolutions per minute for 30 s at approximately 1670 °C. In each evaluation test three prismatic samples were dipped in the steel melt. For the determination of the degree of in situ spinel formation, the diffractometer PANalytical X'Pert PRO MPD 3040/60 (Panalytical/NL) was used concludingly. In this case, the diffraction patterns were recorded within 15°–140°, with steps of 0,013° and a time of 30 s per step. In order to detect a possible dependency of the chemistry of varying filter materials on the deposition of nonmetallic inclusions in steel melt filtration, and their

applicability under industrial conditions, different ceramic foam filters, have been tested. All tested filters were of the size 70 mm × 70 mm × 20 mm and had a pore size of 10 ppi. In order to contaminate the steel melt with either exogenous alumina, or spinel inclusions in an accurately defined way, contaminating filters were installed in front of the active and reactive filters respectively, with a distance of 8 cm within the gate system. Therefore Al_2O_3–C filters with a size of 75 mm × 75 mm × 25 mm and a pore size of 10 ppi, were furnished with 20 g of tabular alumina or alumina-rich spinel, via dipping the filters into a slurry. This ensured a complete and mostly homogeneous covering of the entire filter structure with an inclusion layer. The slurry consisted of either 60 mass-% tabular alumina T60/64 (d_{10} = 3,54 µm, d_{50} = 69,01 µm, d_{90} =190,60 µm), or 60 mass-% alumina-rich spinel AR78 (d_{10} = 3,80 µm, d_{50} = 45,03 µm, d_{90} = 125,20 µm), 40 mass-% deionized water, and 0,3 mass-% (referred to solid content) xanthan as stabilization agent. The filters were dried at 80 °C for 12 h. Due to the absence of a thermal treatment at elevated temperatures, a loosely, easily detachable coating could have been generated. Within this contribution, the cast steel G42CrMo4 (1.7231) was used. The casting trials were accomplished in collaboration with foundry Edelstahlwerke Schmees (Pirna/DE). After the tap at a temperature of 1720 °C, the steel melt was aluminum deoxidized and purged with argon for 3 min. The casting temperature was finally adjusted to 1623 °C and the oxygen content amounted to 5,37 ppm. For subsequent investigations, the cooled, steel filled filters were halved with the aid of water jet cutting and once more subdivided into three parts. Concludingly a polishing process was conducted, in order to generate samples for scanning electron microscopy (SEM) investigations.

Tab. 1 Compositions of the Al_2O_3-C filter [11]

Components [%]	AC5	AC9
Al_2O_3 Martoxid MR 70	66	64
Carbores® P	20	30
Graphite AF 96/97	7,7	3,3
Carbon black MT N-991	6,3	2,7
Additives [%]		
Ligninsulfonate T11B	1,5	1.5
PPG P400	0,8	0,8
Castament VP 95 L	0,3	0,3
Contraspum K 1012	0,1	0,1
Total Solid Content [%]		
Impregnating slurry	83,0	85,7
Spraying slurry	75,6	79,1

3 Results and discussion

3.1 Active filter materials with increased amorphous carbon content

3.1.1 Activation due to resin coating

In order to generate active filters with an high amorphous carbon content, Al_2O_3–C filters (AC5) were spray coated with pure resin in either the green state, or already coked at 800 °C. The mechanical properties of filters with and without active amorphous carbon coating are listed in Tab. 6. It presents the crucial influence of a thermal pretreatment of the filter substrate on the CCS in case of the application of a resin coating. Here, the resin generates macrocracks within the thermally non-pretreated filter substrates (Fig. 1) during the coking process, resulting in the lowest CCS values of 0,22 N/mm². However, the application of the coating on coked filter substrates leads to the remarkable increase of CCS of about 250 %, compared to the uncoated filter substrate. This is traceable back to the infiltration of the substrate by the resin, which, on the one hand, rounds the sharp edges of

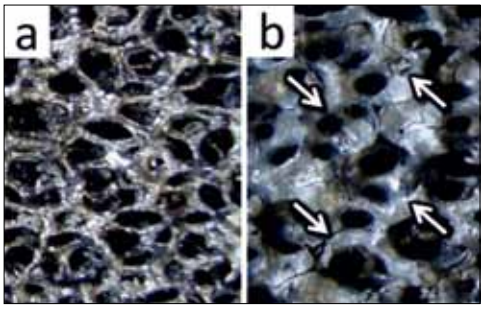

Fig. 1 Resin coated, coked filters with (a) and without (b) thermal pretreatment at 800 °C [15]

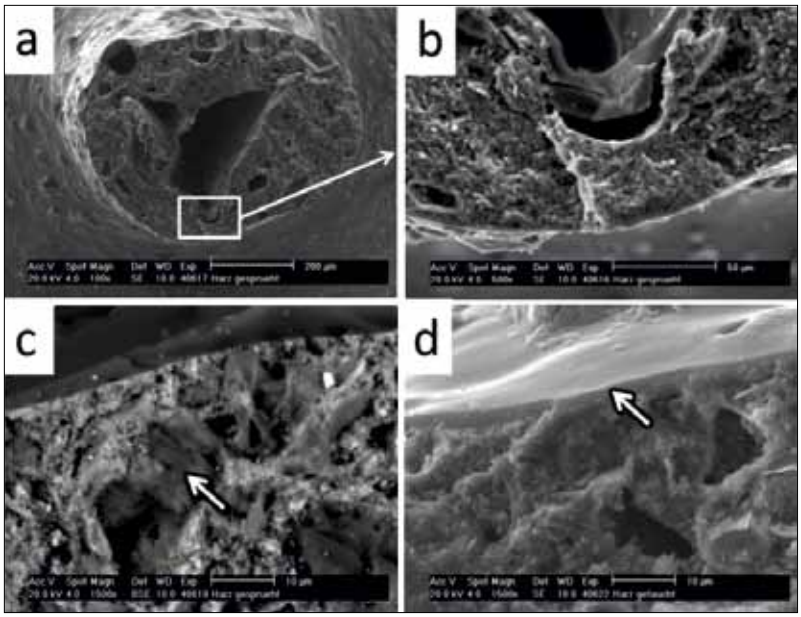

Fig. 2 Resin coating of filter AC5 leads to rounding of the sharp edges of the hollow filter struts (a+b), reduction of the total open porosity (c) and increase of the load bearing cross section (d) [15]

the hollow filter struts, resulting in decreasing stress peaks (Fig. 2a, b). On the other hand, this infiltration reduces the total open porosity of the filter material itself (Fig. 2c), from 35,8 vol.-% (AC5) to 21,5 vol.-% (AC5+Resin). Additionally, the coating, which is chemically bonded, facilitates the healing of defects of the substrate material and increases the load bearing cross section, as shown in Fig. 2d. From Tab. 6 arises that, under consideration of the number of coking steps, the CCS of the uncoated filters do not vary outside standard deviation. It can therefore be stated that the increasing CCS is mostly traceable back to application of the coating, and less to the number of coking steps. Due to the application of the active coating, the Young's modulus increases from 0,40 kN/mm² (AC5) to 1,43 kN/mm² (AC5+Resin) consequentially. It has to be taken into account that the Young's modulus values in this contribution, measured on filter structures, do only serve as comparative values, not as absolute values. Even though a resin coating leads to pure amorphous carbon surfaces after coking at 800 °C, these filters do not possess sufficient thermal shock resistance. Immediately after impingement of the steel, the filters were destroyed, resulting in unhindered metal melt flow. Under consideration of the respective Young's moduli, it appears that, due to the considerably higher Young's modulus in case of the coated filters, the thermal shock resistance decreases accordingly. However, pitches have the ability to convert into more crystalline structures as a result of increasing annealing temperatures. Hence, the following chapter covers the influence of varying coking temperatures on the properties of carbon bonded alumina filters, based on composition AC5.

Tab. 2 Compositions of the oxidic coating of active filters [12]

Components [%]	Alumina Coating	Spinel Coating	Mullite Coating
Alumina CL 370	100	–	–
Spinel AR 78	–	100	–
Mullite SYMULOX M 72 K0	–	–	100
Additives [%] *			
Ligninsulfonate T11B	1,5	1,5	1,5
Castament VP 95 L	0,3	0,3	0,3
Contraspum K 1012	0,1	0,1	0,1
Total Solid Content [%]			
Spraying slurry	65,0	65,0	65,0

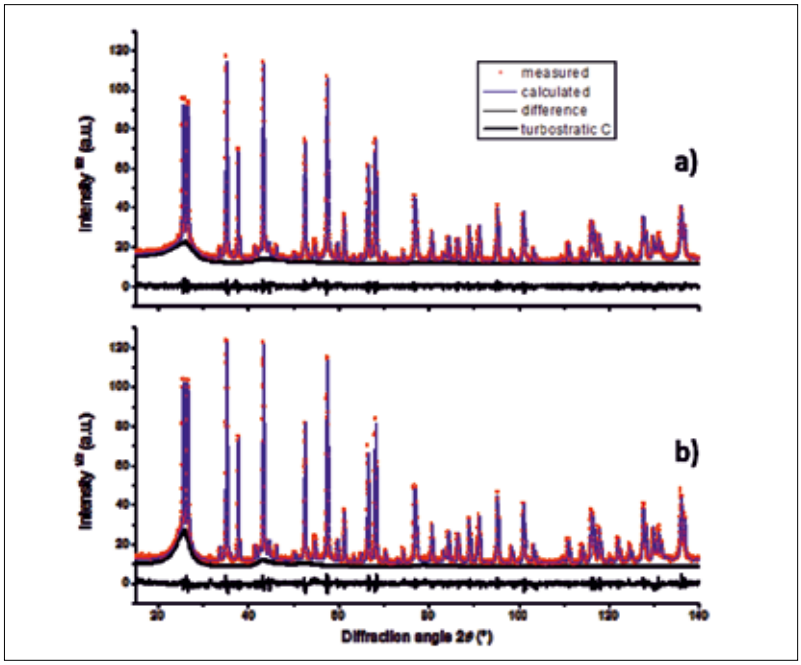

Fig. 3 Measured (dots), refined (lines) and difference (lines at the bottom of each plot) X-ray diffraction patterns of specimens coked at 800 °C (a) and 1400 °C (b). The Carbores® P and carbon black contribution to the diffraction patterns (noted as turbostratic C) is shown as a thick line below the sharp crystalline phase's peaks [15]

3.1.2 Activation due to the variation of coking temperatures

Tab. 7 presents the mechanical properties of both, filters coked at 800 °C and 1400 °C. It is shown that the CCS, as well as the Young's modulus of filters coked at 800 °C, is higher. Taking into account the open porosity of the filter material itself, it becomes clear that the elevated annealing temperature leads to an increasing porosity from 35,02 % (AC5 800 °C) to 40,27 % (AC5 1400 °C). Due to the associated reduction of the load-bearing cross section, the CCS decreases and the Young's modulus declines accordingly. The increase in open porosity is to trace back to further pyrolysis, leading to the evaporation of hydrocarbons. With the aid of X-ray diffraction, only moderate changes in the microstructure of crystalline phases Al_2O_3 and/or graphite in samples coked at 800 °C and 1400 °C were found in studied samples. Lattice parameters of Al_2O_3 were in all specimens under investigation a = 0,4761 ± 0,0001 nm, c = 1,2996 ± 0,0001 nm. In specimens containing graphite, refined lattice parameters were a = 0,2461 ± 0,0001 nm, c = 0,6716 ± 0,0002 nm. Pronounced change in the coherently diffracting domain size was observed in the Al_2O_3 phase. The specimens coked at 800 °C had a crystallite size of approximately 300 nm, while the diffraction peak widths even decreased, which imply the crystallite size growth, in specimens coked at 1400 °C. However, the value of 300 nm is on the edge of the crystallite size estimation using the X-ray diffraction methods, so it can be deduced that the crystallite size of Al_2O_3 particles increased in specimens coked at 1400 °C, but it cannot be quantified, based on the X-ray diffraction measurements only. The mean crystallite size of graphite did not show significant change between specimens coked at 800 °C and 1400 °C and was about

160 nm. Measured and refined X-ray diffraction patterns of specimens coked at 800 °C (a) and 1400 °C (b) are shown in Fig. 3. More pronounced changes in the microstructure between the samples coked at 800 °C and 1400 °C, are in turbostratic carbon phases (i.e. Carbores® P and carbon black). It is experimentally very difficult to separate the contributions of both turbostratic phases to the overall diffraction pattern, since both constituents contribute to very broad and low intensity peaks, which are superimposed with sharp and intensive Bragg peaks from crystalline phases. However, based on studies by Dopita et al. [13] of both pure phases, Carbores® P and used carbon black, annealed at different temperatures, the basic microstructural parameters of carbon black coked at 800 °C are: lattice parameters a = 0,24449 nm, c = 0,70304 nm, the mean cluster sizes are La = 2,53 nm (cluster size in the plane of graphitic layer) and Lc = 2,11 nm (cluster size perpendicular to the graphitic layer). Carbon black annealed at 1400 °C shows lattice parameters a = 0,24474 nm, c = 0,6950 nm, the mean cluster sizes are La = 3,93 nm and Lc = 2,78 nm. Even more pronounced changes in the microstructure i.e. cluster sizes growth and changes in the lattice parameters, were observed in Carbores® P. In Carbores® P, coked at 800 °C, the lattice parameters are a = 0,24397 nm, c = 0,69164 nm and the mean cluster sizes are La = 1,98 nm (cluster size in the plane of graphitic layer) and Lc = 1,38 nm.

Carbores® P, annealed at 1400 °C, yields lattice parameters a = 0,24463 nm, c = 0,6881 nm, the mean cluster sizes are La = 5,32 nm and Lc = 4,82 nm. Under consideration of common values for the cluster sizes of pyrolized pitches (La = 0,3–2 nm, Lc = 1–5 nm) it appears that these values equate to those, generated after annealing at 800 °C. A coking temperature of 1400 °C, however, results in values exceeding the cluster sizes of the semicoke. It can thus be stated that higher coking temperatures lead to decreased isotropy of carbon, aligned with the desired changes in physical properties, which might have influence on the filtration behavior. Due to only minor changes in the CCS as well as in the Young's modulus, the filters coked at 1400 °C pass the impingement test. Therefore, newly developed filters exist, which provide good comparability concerning their respective filtration behavior. As a consequence of the identical compositions of the filters, influencing parameters are effectively minimized to the variation of amorphous (turbostratic) and crystalline carbon modifications [15].

Tab. 3 Compositions of the reactive MgO–C filters [13]

Components [%]	AC5	AC9	MC1	MC2	MC3
Al_2O_3	66	64	–	–	–
MgO	–	–	66	64	63
Carbores® P	20,0	30,0	20,0	30,0	35,0
Graphite	7,7	3,3	7,7	3,3	1,1
Carbon black	6,3	2,7	6,3	2,7	0,9
Additives [%] *					
Ligninsulfonate T11B	1,5	1,5	1,5	1,5	1,5
Castament VP 95 L	0,3	0,3	0,3	0,3	0,3
Contraspum K 1012	0,1	0,1	0,1	0,1	0,1
Total Solid Content [%]					
Impregnating slurry	82,0	83,3	75,5	75,1	–
Spraying slurry	–	–	63,7	68,0	70,8

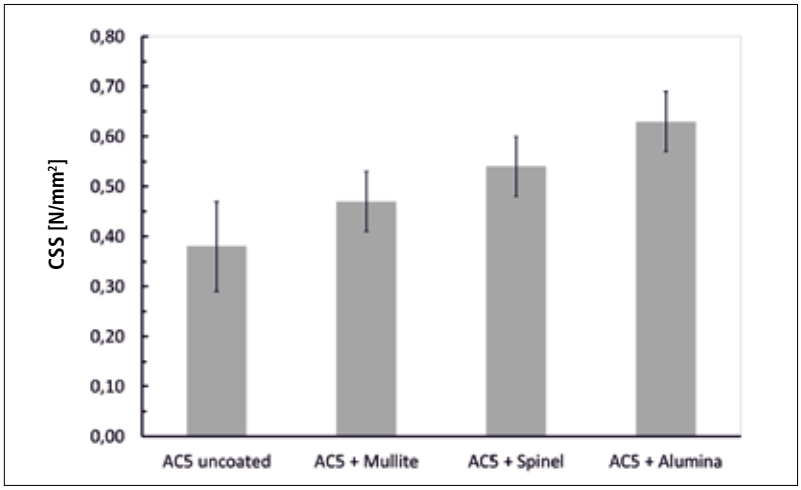

Fig. 4 Cold crushing strengths of the coated and uncoated filter systems, coked at 1400 °C [12]

3.2 Active filter materials with oxide coating

The second approach of activating carbon bonded filters in course of the present work consists of the application of pure oxidic coatings. These allow a defined adjustment of the surface chemistry, surface tensions and surface roughness, which enables the determination of various influencing parameters, concerning the steel melt filtration. The results regarding the influence of the coating on the CCS are illustrated in Fig. 4, which includes thermally pretreated filters, coked at 1400 °C. Based on the application of the coating, the CCS increases from 0,36 N/mm² (uncoated) to 0,47 N/mm² for mullite, 0,54 N/mm² for spinel and 0,63 N/mm² for the alumina coating. Due to the coating, the effective cross section increases slightly, which is accompanied by a reduction of occurring stresses in the struts, proportional to $1/r^3$ and a minimization of the carbon oxidation is expected. Moreover, the shrinkage of the coating onto the filter struts is assumed to generate compressive stresses that counteract the peak stresses of the hollow filter struts, resulting in higher cold crushing strengths. Additionally, compressive stresses occurring during cooling, as follows from Fig. 5, contribute to an increase in CCS. Here, the dilatometer curve of an uncoated filter is opposed to the filters coated with mullite, spinel and alumina re-

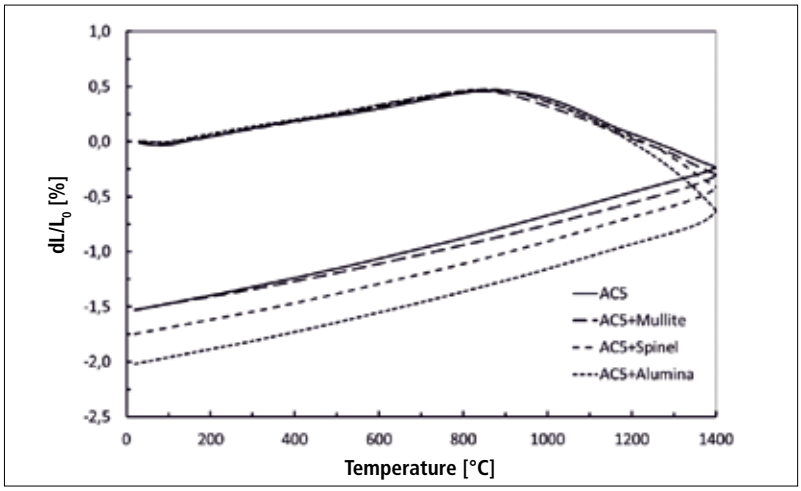

Fig. 5 Shrinkage behavior of the coated and uncoated filters, in situ sintered under argon within the dilatometer [12]

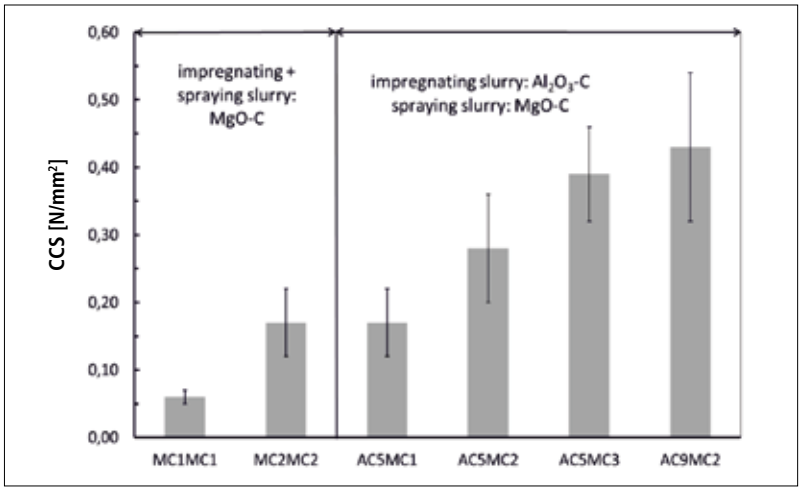

Fig. 6 Cold crushing strengths of the reactive filters, consisting of different layer compositions [13]

spectively, in situ sintered within the dilatometer under inert argon atmosphere. All curves, up to a temperature of approximately 850 °C, show an expansion of 0,5 %, which is attributed to the thermal strain. The following shrinkage behavior of all tested filters is due to a dehydrogenation process of the carbon bonded substrate material, with which most of the remaining volatile components are removed. These are still present up to 800 °C, because of a thermal pretreatment of only 800 °C. Shrinkage is increased besides by a graphitization process, resulting in a higher degree of order of the graphite-like structures. The oxide coated filters present a more pronounced shrinkage within the temperature range of 1150 °C, up to the final temperature of 1400 °C. The varying sintering behaviours of the respective oxides lead to different shrinkage values. Due to the thermal treatment, the oxides shrink onto the substrate material, resulting in tight and microcrack free coatings. Hence, the dependence of the CCS increase, as a function of the coating material, correlates exactly with the shrinkage. With an increasing amount of shrinkage, the porosity is decreased while compressive stresses are increased, which leads to the highest CCS for alumina and the lowest CCS for mullite. Due to nearly same coating thicknesses, other influencing factors are mainly eliminated [12]. The accomplishment of the impingement test verified the applicability of the newly developed filter materials. Therefore, thermally pretreated filters (800 °C), coated with the respective oxides, sintered at 1400 °C have been tested. It followed that the respective coatings still remain after the test, due to the high thermal conductivity of the carbon bonded substrate material and coating thicknesses of only approx 60 µm, which compensates the poor thermal shock resistance of the oxide coating materials. Moreover, stress peaks appearing at the triconcave, hollow filter struts are reduced by the coatings [12].

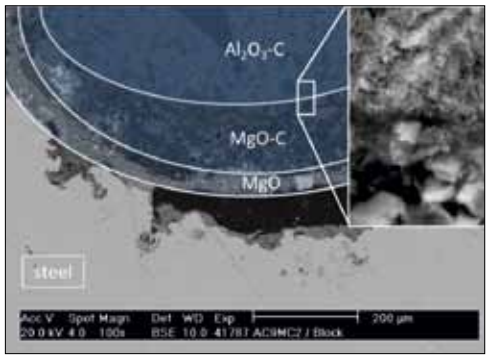

Fig. 7 SEM image of filter AC9MC2 after passing the impingement test at 1670 °C [15]

3.3 Reactive filter materials

The cold crushing strengths of the respective filter compositions are presented in Fig. 6. From this it follows that the pure MgO–C (MC) based compositions MC-1MC1 and MC2MC2 exhibit only low CCS. Even a high binder amount of 30 mass-% does not result in CCS above 0,18 N/mm² and is accompanied by the appearance of macrocracks. This is due to the fact that MgO has a higher thermal expansion coefficient than carbon; the matrix is stressed and deformed. During cooling, the oxides exhibit a more pronounced shrinkage, resulting in porosity formation around the oxide particles. This means that the greater the thermal expansion of the oxide, the larger the pore volume, the lower the CCS. The second factor of influence is the particle size. Since there is no chemical bonding between the oxide particles and the carbon matrix, but only mechanical interlocking, the interface forms the critical crack length. With increasing particle size, this crack length increases; this could be observed from the comparison of CCS due to the use of fine grained alumina, as well as from the partial substitution of magnesia by alumina. Hence, a layer construction has been developed, consisting of an impregnating layer based on Al_2O_3–C (AC) and a spraying layer based on MgO–C (MC). This resulted in remarkably improved mechanical properties,

without influencing a possible reactive function on the filters surface [13]. The results of the impingement tests are exemplarily represented by layer composition AC-9MC2 in Fig. 7. All filters with the carbon bonded alumina substrate and with the carbon bonded magnesia coating survived the impingement test. The carbon bonded MgO coating is still remaining on the carbon bonded Al_2O_3 substrate without any crack generation or delamination. The image enlargement presents the interface between the coatings. The bigger MgO grains in comparison to the smaller Al_2O_3 can be registered. It can be seen that due to the application of the same type and amount of the binder no cracks, as well as no delamination of the two coatings could be identified at the interface after coking as well as after thermal shock. However, a new coating consisting of pure MgO was formed. This can be attributed to two possible mechanisms of action. On the one hand, the surface could have been partially decarburized up to a depth of approximately 20 µm. On the other hand, secondary MgO could have been formed, as a consequence of the carbothermal reduction [12].

Tab. 4 Layer compositions for the development of MgO–C filters [13]

Combination	Impregnating Slurry (Approx. 50 mass-% of the Filter)	Spraying Slurry (Approx. 50 mass-% of the Filter)
MC1MC1	MC1	MC1
MC2MC2	MC2	MC2
AC5MC1	AC5	MC1
AC5MC2	AC5	MC2
AC5MC3	AC5	MC3
AC9MC2	AC9	MC2

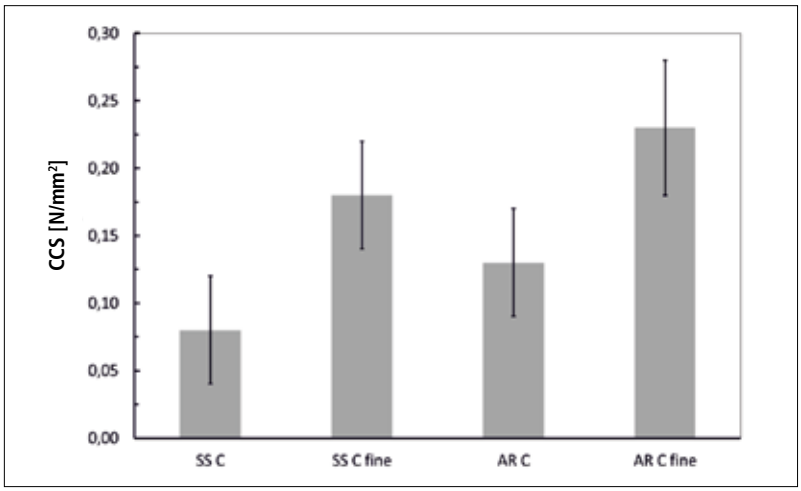

Fig. 8 Cold crushing strengths of 10 ppi filters produced using particles of different size, after a thermal treatment at 800 °C [14]

3.4 Combined active and reactive filters

The cold compression strength, measured on the various combined filters coked at 800 °C, is reported in Fig. 8. Magnesia seems to have a detrimental effect on the CCS, as filters with the higher amount of MgO (SS-C) lead to lower average strength (0,08 N/mm²), compared to AR-C (0,13 N/mm²). This is in good accordance with the CCS values of pure MgO–C, as well as Al_2O_3–C filters, based on a comparable composition, as shown in chapters 3.1 and 3.3. The highest CCS is achieved when using only alumina (0,39 N/mm²), whereas pure magnesia leads to the lowest CCS (0,06 N/mm²). As already described, this is predominantly traceable back to both, the larger particle sizes and the greater thermal expansion coefficient of MgO. [14] Due to the higher CCS, only the compositions produced using fine alumina, heated only at 800 °C, were tested by dipping in the steel melt. As it can be seen in Fig. 9 (b, d), both SS-C fine and AR-C fine samples exhibit

Tab. 5 Compositions of the combined MgO–Al_2O_3–C materials [14]

Components [%]	SS-C	SS-C Fine	AR-C	AR-C Fine
Al_2O_3 fine or coarse	47,3	47,3	51,5	51,5
MgO	18,7	18,7	14,5	14,5
Carbores® P	20,0	20,0	20,0	20,0
Graphite	7,7	7,7	7,7	7,7
Carbon black	6,3	6,3	6,3	6,3
Additives [%] *				
Ligninsulfonate T11B	1,5	1,5	1,5	1,5
Castament VP 95 L	0,3	0,3	0,3	0,3
Contraspum K 1012	0,1	0,1	0,1	0,1
Total Solid Content [%]				
Impregnating slurry	80,0	80,0	80,0	80,0
Spraying slurry	70,0	70,0	70,0	70,0

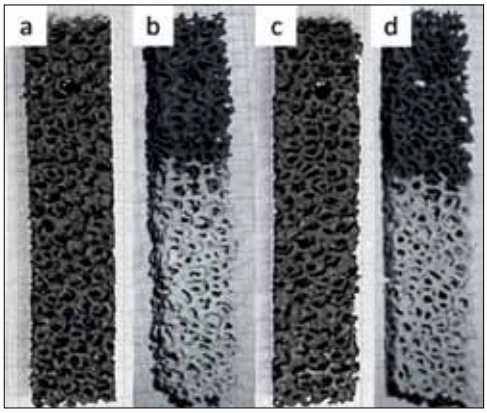

Fig. 9 Samples before and after dipping into the steel melt at 1640 °C: (a) SS-C fine coked at 800 °C; (b) SS-C fine after dipping; (c) AR-C fine coked at 800 °C; (d) AR-C fine after dipping [14]

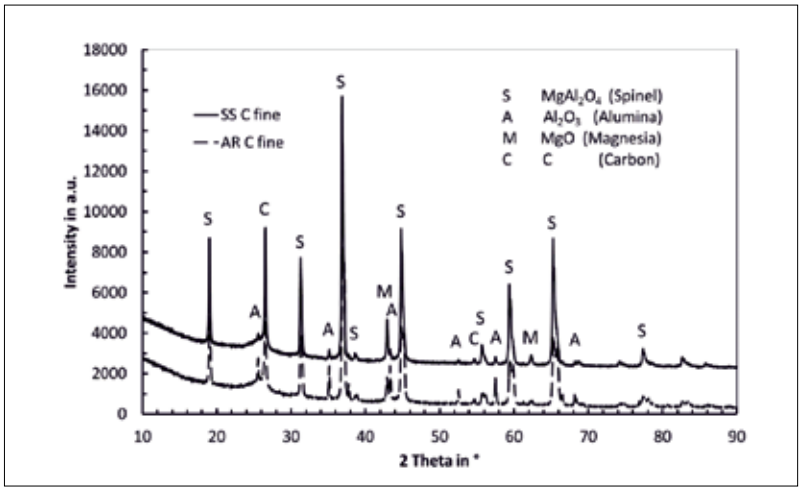

Fig. 10 Phase evolution for samples AR-C fine and SS-C fine after dipping in the steel melt at 1640 °C [14]

Tab. 6 Mechanical properties of resin coated and uncoated filters, based on composition AC5, with and without thermal pretreatment at 800 °C [15]

		Coking at 800 °C (Without Thermal Pretreatment)	Coking at 800 °C (With Thermal Pretreatment)
CCS [N/mm²]	AC5	0,39 ± 0,06	0,36 ± 0,04
	AC5+Resin	0,22 ± 0,07	0,90 ± 0,19
Young's modulus [kN/mm²]	AC5	0,41 ± 0,17	0,40 ± 0,23
	AC5+Resin	–	1,43 ± 0,14

Tab. 7 Mechanical properties of filter composition AC5, coked at 800 °C or 1400 °C [15]

	Coking at 800 °C	Coking at 1400 °C
CCS [N/mm²]	0,39 ± 0,06	0,33 ± 0,14
Young's modulus [kN/mm²]	0,41 ± 0,17	0,33 ± 0,12

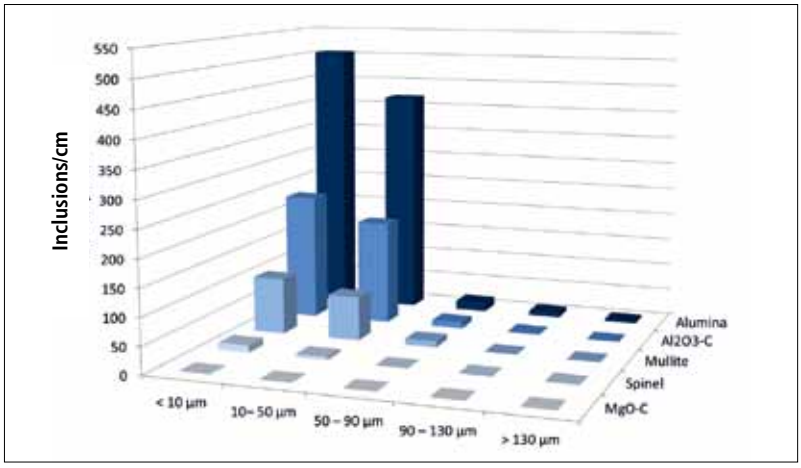

Fig. 11 Amount of trapped exogenous alumina as a function of filter chemistry [17]

sufficient thermal shock resistance. Within the 30 s of contact with the steel melt (1640 °C), which matches the approximate casting time, no macrocracks form or spalling occurs. The discoloration of the filters surface at the contact with the molten steel is due to surface decarburization on the one hand, and to a newly formed coating on the other hand. The X-ray diffraction analysis enabled to assess the phase evolution of the filters immersed in the steel melt (Fig. 10). As it can be seen, most of the reactants convert into spinel, with only small amounts of MgO and Al_2O_3 still remaining for both compositions [14].

3.5 Influence of chemistry of the respective filters on the filtration of alumina inclusions

With regard to the filtration behavior towards exogenous alumina inclusions as a function of chemistry of the respective filters, the direct comparison of all tested filters presents distinctive differences (Fig. 11). The alumina coated filters possess the highest affinity towards alumina based nonmetallic inclusions. In general, the particle sizes of the trapped exogenous alumina inclusions equate to the initial particle size distribution. The carbon bonded alumina filter leads to the second best filtration results, which consists of at least 69 mass-% pure alumina. The mullite, as well as the spinel coated filters, present a worse filtration behavior. With regard to the mechanical properties of the filtered steel, Henschel et al. have certified the current filtration results concerning mullite coated, as well as uncoated, Al_2O_3–C filters [16]. Here, they came to the conclusion that mechanical properties of steel can be even more improved due to the application of carbon bonded alumina filters, compared to the application of mullite coated filters. Due to the absence of alumina in the reactive MgO–C filter system, nearly no pure exogenous alumina inclusions are trapped. This leads to the assumption that the chemistry of the respective carbon bonded oxide exhibits great influence on the attraction forces between filter material and nonmetallic inclusion, in contrast to the amorphous carbon bonding itself [17].

3.6 Influence of chemistry of the respective filters on the filtration of spinel inclusions

The filtration behavior of the varying filter materials towards exogenous spinel inclusions is illustrated in Fig. 12. The data received show that considerably less spinel inclusions have been trapped, in comparison to the filtration results concerning alumina inclusions. According to Dekkers, spinel inclusions are assumed to possess fewer tendencies to separate from the li-

quid steel at the slag-steel or the refractory-steel interface. Moreover, comparably lower surface energies of spinels are expected to exhibit decreased agglomeration rates, which result in less pronounced harmfulness, reflected in improved mechanical properties of the steel [18]. In terms of the influence of the filter chemistry on the filtration of spinels, a similarity with that of alumina becomes apparent. Here, too, it is seen that the alumina coated filter (AC5 + Alumina) leads to the best filtration results and the reactive MgO-C filter (AC9MC2) to the worst. However, the differences in the amount of trapped particles between the respective filters are less pronounced, which might be traced back to generally less filtered particles. As aforementioned, the varying surface energies and thus, increasing interfacial energies are strongly suggestive to be the reason for the efficient filtration behavior of alumina filters [15].

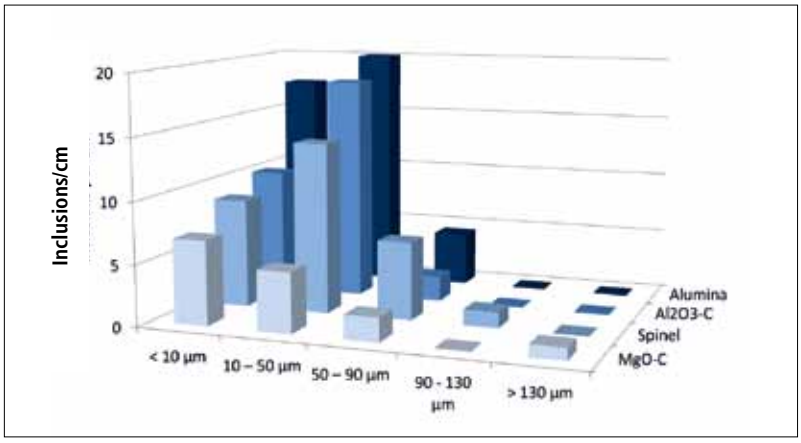

Fig. 12 Amount of trapped exogenous spinel as a function of filter chemistry [15]

4 Conclusions

The development of filter materials for steel melt filtration, based on carbon bonded alumina, was achieved in the present work. These filters served as substrates for further functionalization processes in terms of so-called active filters. In order to functionalize the carbon bonded alumina filter via increasing amorphous carbon amounts, filters of the type AC5 were spray-coated with resin, in order to generate pure amorphous carbon surfaces. The resin infiltrated the pores of the thermally pretreated filters, resulting in decreasing open porosity, increasing cold crushing strengths, as well as increasing Young's modulus of elasticity and thus, in poor thermal shock resistance. Hence, the influence of varying coking temperatures on the properties of carbon bonded alumina filters, based on composition AC5 was determined. Only minor changes in the CCS, as well as in the Young's modulus of the filters, coked at 1400 °C occurred. This led to the pass of the impingement test. In terms of the second functionalization approach, new active oxide coated filters for steel melt filtration, with a coating thickness of approx. 50-80 µm, have been developed. A sintering temperature of 1400 °C led to the generation of tight coated filter systems, due to a pronounced shrinkage of the coating materials onto the filter struts. In addition, the sintering, as well as the cooling shrinkage, generated compressive stresses that counteract the peak stresses of the hollow filter struts, resulting in higher cold crushing strengths. The amount of the CCS increase was dependent on the sintering activity of the respective oxides. Therefore, the CCS decreased from alumina over spinel to mullite. Concludingly, the applicability of the newly developed filter systems in consideration of their thermal shock resistance, as well as their permeability, was approved. Despite the fact that MgO is susceptible to hydration, leading to brucite formation, the application of thin, water based coatings, on carbon bonded alumina substrates, was possible, resulting in reactive MgO–C filters. As a result of the low packing densities, the bigger particle sizes and the pronounced thermal expansion coefficient, these filters possessed very low cold crushing strengths, as well as no dimension stability. Hence, the production of pure magnesia containing filters had been proven to be impractical. Therefore, the carbon bonded alumina composition was used as a first, impregnated layer. In combination with a MgO–C spraying layer, stable filters with a wall thickness distribution of 400–600 µm (±330 µm), which passed the impingement test, were generated. In order to combine the functionalities of the active and reactive filters and to exploit the volume expansion of the in situ spinel formation, filters, based on the system MgO–Al_2O_3–C were produced. The formation of spinel reduced the overall shrinkage of the ceramic materials, which is detrimental in filtration applications because it reduces the permeability of the filters. The data prove that these innovative systems can be successfully used for molten steel filtration.

Finally, a selection of newly developed filters was tested in collaboration with the industry. Within the scope of the present work the influence of the chemistry of varying filter materials on the filtration of exogenous alumina, as well as spinel inclusions has been verified. That implies that the higher the alumina amount on the surface is present in the filter system, the more nonmetallic inclusions are getting trapped on the filter surface.

References

[1] Bargel; H.-J.; Schulze, G.: Eisenwerkstoffe. Werkstoffkunde. Berlin, Heidelberg, New York 2005, 141–268

[2] Jacobi, H.: The process metallurgy and materials engineering of steel with high purity and cleanness. Feuerfeste Werkstoffe und Systeme für die Erzeugung hochreiner Stähle. In: Proceedings of XXXVII. Int. Feuerfest-Kolloquium, Stahl und Eisen Special (1994) 5–16

[3] Yang, W.; et al.: Nucleation, growth, and aggregation of alumina inclusions in steel. JOM **65** (2013) [9] 1138–1144

[4] Holappa, L.; Wijk, O.: Inclusion engineering in treatise on process metallurgy. Industrial Processes **3** (2014) 347–372

[5] Uhrus, L.O.: Through-hardening steels for ball bearings – effect of inclusions on endurance. Iron Steel Inst., Spec. Rep. **77** (1963) 104–109

[6] Janke, D.; Raiber, K.: Grundlegende Untersuchungen zur Optimierung der Filtration von Stahlschmelzen. Technische Forschung Stahl, Luxembourg: Europäische Kommission, 1996, ISBN 9282764583

[7] Hammerschmid, P.; Janke, D.: Kenntnisstand zur Abscheidung von Einschlüssen beim Filtrieren von Stahlschmelzen. Stahl und Eisen **108** (1988) [5] 211–219

[8] Hammerschmid, P.; Raiber, K.; Janke, D.: Abscheidung von Tonerdeeinschlüssen aus Stahl- und Nickel-Basis-Schmelzen mit keramischen Filtern. Konferenz-Einzelbericht: Stahl und Eisen Special (1994) 58–64

[9] Morales, R.D.; et al.: Computer and fluid flow modeling of filtration mechanisms in foam filters. Transa. Amer. Foundry Soc. (2008) 715–731

[10] Schwartzwalder, K.: Method of making porous ceramic articles. In: Patent US 3090094 (1963)

[11] Emmel, M.; Aneziris, C.G.: Development of novel carbon bonded filter compositions for advanced steel melt filtration. Ceramics Int. **38** (2012) [6] 5165–5172

[12] Emmel, M.; Aneziris, C.G.: Functionalization of carbon-bonded alumina filters through the applications of active oxide coatings for the steel melt filtration. J. of Mater. Research **28** (2013) [17] 2234–2242

[13] Aneziris, C.G.; et al.: Reactive filters for steel melt filtration. Adv. Engin. Mater. **15** (2013) [1–2] 46–55

[14] Emmel, M.; et al.: In situ spinel formation in Al2O3-MgO-C filter materials for steel melt filtration. Ceram. Int. **40** (2014) [8] 13507–13513

[15] Emmel, M.: Development of active and reactive carbon bonded filter materials for steel melt filtration. PhD thesis, Technische Universität Bergakademie Freiberg (2014)

[16] Henschel, S.; et al.: Effect of filter coating on the quasi-static and cyclic mechanical properties of a G42CrMo4 casting. Adv. Engin. Mater. **15** (2013) [12] 1216–1223

[17] Emmel, M.; et al.: Influence of the chemistry of ceramic foam filters on the filtration of alumina based non-metallic inclusions. Adv. Engin. Mater. **15** (2013) [12] 1188–1196

[18] Dekkers, R.: Non-metallic inclusions in liquid steel. PhD thesis, Katholieke Universiteit Leuven, Belgium, 2002